Proceedings of the 11th ICPMG 2026
11th International Conference on Physical Modelling in Geotechnics
8-12 June 2026, Zurich, Switzerland

Centrifuge Modeling of Face Stability in Shallow TBM Excavations in Cohesionless Soils

A.F. Durand
Norte Fluminense State University, Campos dos Goytacazes, Brazil, aldo@uenf.br

F. Saboya, S. Tibana, C. Cabral
Norte Fluminense State University, Campos dos Goytacazes, Brazil, saboya@uenf.br, tibana@uenf.br

C. Cabral
Norte Fluminense State University, Campos dos Goytacazes, Brazil, cleitoncabraleng@gmail.com

ABSTRACT: Tunnel face stability in sandy soils was investigated using geotechnical centrifuge modelling. A half-section tunnel model was tested under 50g acceleration, with excavation simulated in a controlled manner using a movable piston. Surface settlements and internal displacement fields were measured via Digital Image Correlation (DIC) and Particle Image Velocimetry (PIV). The experimental results demonstrate the significant influence of soil density and cover-to-diameter ratio (C/D = 0.5, 1.0, and 2.0) on failure mechanisms. In loose sands, broad collapse chimneys extended to the ground surface, whereas dense sands exhibited localized wedge-type failures governed by soil arching effects. Empirical correlations between surface settlement and required face support pressure were established, providing practical guidance for the design and operation of Earth Pressure Balance (EPB) shield tunneling. These findings contribute to improved design criteria for shallow tunnel construction in granular soils, promoting face stability and minimizing surface deformations.

1 INTRODUCTION

Initially developed in Japan and later adopted worldwide, geotechnical centrifuge modeling has been established as a robust experimental technique since the 1980s. The number, scale, and simulation capacity of centrifuge facilities have continued to expand, particularly in China (Ng, 2014). This methodological process has paralleled the growing demand for urban infrastructure in densely populated metropolitan areas, where surface space is severely limited. In this scenario, subsurface development has become a key strategy, with tunnel construction for transportation systems, sanitation, and utility networks providing an effective means of increasing urban capacity while minimizing surface disruption, preserving existing structures, and improving mobility.

Improved understanding of underground structures is especially critical for mechanized excavation technologies, such as Earth Pressure Balance Tunnel Boring Machines (EPB-TBM.). According to Zare Naghadehi et al. (2019), the two primary TBM types used in soils are slurry pressure balance shields (SPB) and earth pressure balance shields (EPB), with selection governed by geotechnical and geological factors including soil type and variability, hydrogeological conditions, and excavation depth. The performance of these systems is closely linked to pressure control within the working chamber, essential for maintaining face stability and limiting surface settlements.

Comparative studies on settlement patterns reveal marked differences between excavation methods. In open-face excavations, such as those using the New Austrian Tunnelling Method (NATM), surface settlements at the tunnel face may reach approximately 50% of the final maximum settlement. By contrast, tunnels excavated with closed-face EPB-TBMs typically exhibit significantly lower values of 25 to 30% (Mair and Taylor, 1997, cited in Saldivar, 2024).

Determining the optimal face support pressure poses a complex challenge in geotechnical engineering. As noted by Indiger et al (2011), constructing shallow tunnels in soil using EPB-TBMs requires a carefully balanced support system. Insufficient pressure may lead to face instability and collapse, whereas excessive pressure can result in blow-out events or ground heave, in addition to incurring high costs associated with maintaining support pressures proportional to the geostatic stress gradient. Furthermore, Kirsch (2010) emphasizes that face stability is a fundamental requirement not only for controlling surface deformations, but also for preventing progressive ground failure ahead of the tunnel

Within this framework, the present study investigates soil-tunnel interaction mechanisms during EPB-TBM excavation through physical modeling in a geotechnical centrifuge. The experimental setup enables continuous monitoring of face support pressure during controlled excavation at a constant advance rate, thereby reproducing realistic in-situ stress conditions and three-dimensional excavation effects. Ultimately, the study aims to generate parametrized experimental data that enhance understanding of the mechanisms governing settlement patterns ahead of shallow tunnels excavated in granular soils

2 METHODOLOGY

2.1 Geotechnical Centrifuge Modelling

The experimental program was carried out using the geotechnical centrifuge at the UENF Laboratory under centrifugal acceleration of 50g. Centrifuge modeling is essential for satisfying physical similarity laws because it reproduces stress levels in the reduced-scale model equivalent to those in the full-scale prototype, thereby minimizing scale effects.

2.2 Material Selection and Similarity Criteria

Particle size plays a key role in governing particle motion, since coarser particles form the load-bearing skeletal structure and are the last to become unstable (Wan et al, 2024). Material selection and structural scaling were conducted in strict accordance with the ISSMGE TC104 guidelines for physical modeling in geotechnical engineering. A critical assessment of the ratio between the model tunnel diameter (D) and the mean grain size (d_{50}) yielded a value of approximately 211. Standard dry IPT sand (*Instituto de Pesquisas Tecnológicas do Estado de São Paulo*) was used, with minimum and maximum void ratios of 0.67 and 0.92, respectively. This ratio ensures representative soil-structure interaction, enabling reliable extrapolation of experimental results to the prototype scale while minimizing distortions associated with grain size effects. Table 1 summarizes the density parameters obtained using the pluviation method for loose and dense sand conditions.

Table 1. Index properties of loose and dense sand.

	ρ_{meam} (g/cm^3)	e	Dr (%)
Loose sand	1.46	0.82	39
Dense sand	1.58	0.68	94

2.3 Model Geometry and Experimental Setup

Figure 1 presents the configuration of the centrifuge model. The experiments were conducted in a rectangular container with plan dimensions of 700 x 300 mm and a height of 600 mm. The container features an acrylic viewing window, whose internal surface, in direct contact with the soil mass, defines the model's vertical plane of symmetry. The transparent window enables high-resolution photography for subsequent particle image velocity (PIV) analyses.

The tunnel was modeled with a circular cross-section. To enhance instrumentation efficiency and visual access, while leveraging the axial symmetry of the problem, a semi-circular section (half-section) of the tunnel was constructed. This half-section was positioned flush against the transparent side wall of the container (Figure 1a), which serves as the symmetry plate, thereby minimizing boundary effects associated with container side walls.

A semicircular moveable plate was installed at the tunnel face (Figure 1b). Controlled displacement of this plate provides an analogue for the advancement of the tunnel boring machine (TBM) cutterhead during excavations.

2.4 Excavation Simulation Mechanism

Excavation was simulated by the controlled retraction of the face plate (Figure 1). An external propulsion system, driven by a stepper motor, imposed a constant displacement velocity of 0.008 mm/s. Piston displacement was continuously monitored using a linear variable differential transformer (LVDT). This mechanism enables simulation of the gradual reduction in face support pressure during tunnel advancement.

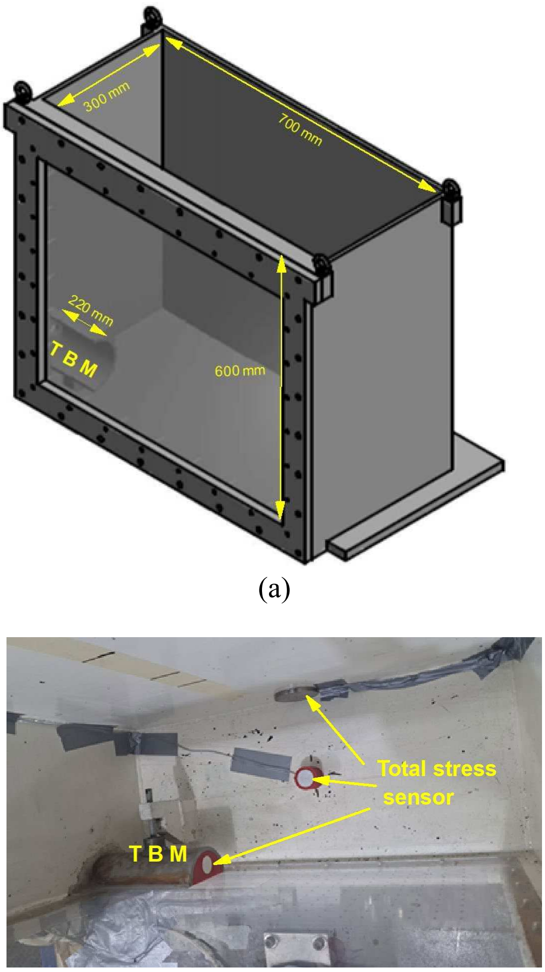

(a)

(b)

Figure 1: Steel container with an acrylic viewing window and the TBM model positioned adjacent to the acrylic wall. (a) General view of the container and its dimensions. (b) Layout of total stress sensors installed on the TBM face plate, at the container base, and along the container side wall (upper view).

2.5 Experimental Program and Instrumentation

Tunnel face failure was investigated under loose and dense sand conditions for three cover depths, expressed as cover-to-diameter (C/D) ratios: 0.5, 1.0, and 2.0. Six centrifuge tests were performed, comprising three tests for each soil relative density. The soil mass response was monitored using a comprehensive instrumentation setup, including total stress sensors to measure vertical and horizontal stresses, LVDTs for localized displacement measurements, and a series of high-resolution photographs captured through the acrylic wall.

Continuous visual recordings were obtained during centrifuge testing using a strategically positioned camera, which served as the basis for displacement field analysis using Digital Image Correlation (DIC). Photogrammetry is a widely used non-intrusive technique for measuring displacements at the ground surface and in the vicinity of tunnels. Numerous studies have demonstrated the effectiveness of Particle Image Velocity (PIV) for geotechnical applications (Megueid et al., 2008). A set of section profiles (S_1, S_2, and S_3) was defined for quantitative evaluation of DIC-derived settlements, as shown in Figure 2.

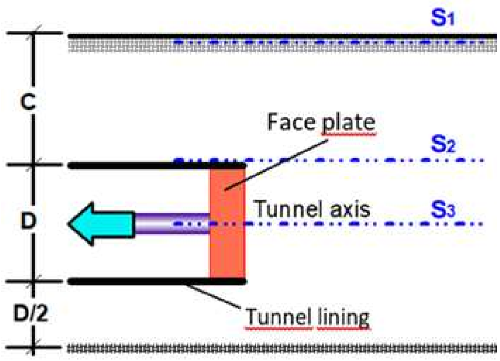

Figure 2: Schematic of the experiment showing the location of the tunnel boring machine (piston) and definition of the settlement monitoring sections (S1, S2, and S3).

3 RESULTS

3.1 Settlements

In this test, the sandy soil was prepared to replicate the prototype geostatic stress state. When the model reached a centrifugal acceleration of 50g, the accurate reproduction of geostatic stresses was confirmed by readings from the total stress sensors.

The unloading phase was initiated under a constant gravitational field. During this phase, a piston representing the TBM face support pressure (red semicircular component shown in Figure 1b) was retracted at a constant velocity of 0.008 mm/s). This simulates material removal during actual tunnel excavation, inducing stress relief at the tunnel face and enabling evaluation of the model's geotechnical response.

Throughout the test, a camera positioned in front of the acrylic wall continuously recorded the model's response under the applied loading conditions. The video recordings were processed into static images based on the actuator velocity. Frames were systematically extracted at intervals corresponding to piston displacements of 0.5 mm, producing a sequence of high-resolution digital images. This dataset enabled detailed analysis of displacement fields and provided a comprehensive view of soil behavior during excavation.

Tunnel-induced settlements were quantified by DIC. Vertical displacement (settlement) profiles were obtained at the instrumented sections (Figure 1) using the Ncorr software implemented in MATLAB (Blaber & Antoniou, 2017), encompassing both soil density conditions investigated (loose and dense sand) and all three C/D ratios.

Figure 3 presents the settlement field distribution (δ) for excavation in loose sand under shallow cover conditions (C/D = 0.5). Maximum settlements occur at the tunnel crown (section S2) and decrease progressively toward the ground surface. The zone of influence of excavation-induced settlements extends approximately half a tunnel diameter ahead of the tunnel face.

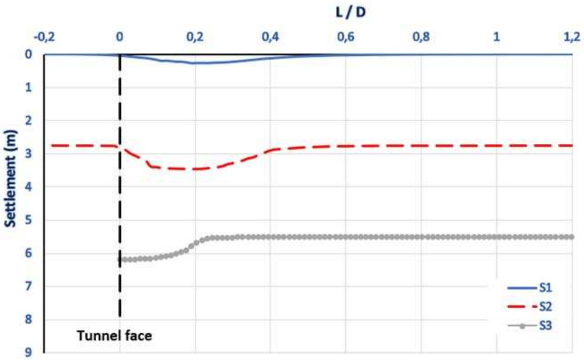

Figure 3: Settlement measurements obtained using the Ncorr MATLAB program for a piston displacement equivalent to 5% of the tunnel diameter (5%D). The curves represent settlements measured at the ground surface (S1), at the tunnel crown (S2), and along the tunnel axis (S3).

A total of six settlement profiles were obtained, each analogous to the profile shown in Figure 3. Based on these results, empirical relationships were derived relating the maximum surface settlement to the C/D ratio for each soil condition, as summarized in Figure 4. The settlement corresponding to profile S_1, located at the ground surface, was used for curve fitting, resulting in the following expressions:

For loose sand:

$$(\delta/D) = [0.0782/(C/D)]^{1.72} \quad (1)$$

For dense sand:

$$(\delta/D) = [0.2024/(C/D)]^{3.77} \quad (2)$$

Where:

C is the cover-to-diameter ratio and δ the surface settlement.

A power-law regression model provided a good fit to the experimental data, with coefficients of determination (R^2) exceeding 0.90. However, it is important to emphasize that each fitted curve was calibrated using only three experimental data points per soil condition. Consequently, the robustness of these empirical relationships can be enhanced by including additional data from future experiments

The relationship between horizontal stress relief measured at the excavation face and the maximum surface settlement was also examined, revealing a linear correlation between these variables, as shown in Figure 5. The corresponding fitted model (Eq. 3), which exhibits a coefficient of determination close to unity, accounts not only for the TBM face pressure, but also the cover depth and unit weight of the ground.

$$[p/(C\gamma)] = 5.0985(\delta/D) + 0.0436 \quad (3)$$

Where:

p is the pressure acting on the excavation shield (TBM head), C the cover depth, and γ the unit soil unit weight.

3.2 Velocimetry

Particle image velocity (PIV), implemented via DIC in MATLAB, was used to quantify the displacement field of the soil mass. This technique enables high-spatial-resolution displacement measurements at thousands of points across the model simultaneously.

Figure 6 shows the velocity field induced ahead of the excavation face for a piston retraction corresponding to 0.5% of the tunnel diameter, with velocity vectors presented for all six experimental scenarios. Qualitative assessment of these fields demonstrates that the mobilized soil zone ahead of the tunnel face is substantially larger in loose than in dense sands, regardless of the C/D ratio. This behavior is consistent with trends reported in previous studies (Idenger et al., 2011).

For the largest cover depth (C/D = 2.0), soil mobilization results in the formation of a localized wedge that does not reach the ground surface. Consequently, surface settlements are negligible, indicating that stress redistribution is primarily governed by internal soil rearrangement and the activation of arching effects in the frontal region of the excavation. The influence of the wedge is even more limited in dense sand conditions, with no direct interaction with the ground surface, as shown in Figures 4 and 5.

4 CONCLUSIONS

This study employed a geotechnical centrifuge to experimentally investigate tunnel face collapse mechanisms and face support pressure requirements for shallow tunnels excavated in sandy soils. The findings can be summarized as follows:

Effect of Soil Density: Dense sand conditions produced narrow and well-defined failure mechanisms. By contrast, low-density sands exhibited significantly wider mobilized soil chimneys, particularly near the ground surface, as revealed by velocity field analysis using Digital Image Correlation (Figure 6).

Effect of Cover Depth (C/D): For an excavation advance equivalent to 5% of the tunnel diameter, simulated by piston retraction, collapse mechanisms propagated to the ground surface at C/D ratios of 0.5 and 1.0. At higher C/D ratios, soil mobilization was confined to a localized wedge adjacent to the tunnel face, with no surface manifestation, confirming the stabilizing role of soil arching. As shown in Figure 5, stress relief at the excavation face exhibits a clear linear relationship with maximum surface settlement, quantified by Eq.3.

Face Support Pressure: Analysis of the empirical relationships in figures 4 and 5 indicates that the minimum support pressure required for face stability increases directly with cover depth. Equation 3 highlights a linear relationship between surface settlement and reductions in face support pressure.

Validation of the Failure Mechanism: The failure mechanism was validated using Digital Image Correlation, which captured a chimney-type collapse pattern consistent with those reported by Chambon & Corte (1994), Idinger et al (2011), Mollon (2009) and Wan (2024). In this mechanism, failure initiated vertically at the tunnel edges, followed by sudden collapse of the soil column, extending approximately 0.5D ahead of the tunnel face. This pattern was consistently observed across all tested C/D ratios (0.5, 1.0, and 2.0).

ACKNOWLEDGEMENTS

The authors are grateful for the financial support of the Fundação Carlos Chagas Filho de Amparo à Pesquisa do Estado do Rio de Janeiro FAPERJ. This research was supported under grant number **E-26/211.804/2021.**

REFERENCES

Blaber J. and Antoniou A. (2017). Ncorr Instruction Manual – Version 1.2.2. *Georgia Institute of Technology*.

Chambon, P. and Corte, J.F. (1994). Shallow tunnels in cohesionless soil: Stability of tunnel face. *Journal of Geotechnical Engineering*, Vol. 120(7): 1148-1165.

IDINGER, G.; AKLIK, P.; WU, W.; BORJA, R. I. (2011). Centrifuge model test on the face stability of shallow tunnel. *Acta Geotechnica*, [S.L.], v. 6, n. 2, p. 105-117, Springer Science and Business Media LLC. http://dx.doi.org/10.1007/s11440-011-0139-2.

KIRSCH, A. (2010). Experimental investigation of the face stability of shallow tunnels in sand. *Acta Geotechnica*, [S.L.], v. 5, n. 1, p. 43-62, 6 mar. 2010. Springer Science and Business Media LLC. http://dx.doi.org/10.1007/s11440-010-0110-7.

Meguid M.A., Saada O., Nunes M.A.1, Mattar J.. (2008). Physical modelling of tunnels in soft ground: A review. Tunnelling and Underground Space Technology 23 (2008) 185–198.

Mollon, G., Dias, D., Soubra, A. H. (2010). Rotational failure mechanisms for the face stability analysis of tunnels driven by a pressurized shield. *Int. J. Numer. Anal. Meth. Geomech*. 2011; 35:1363–1388.

NG, Charles W. W. (2014). The state-of-the-art centrifuge modelling of geotechnical problems at HKUST. Journal Of Zhejiang University Science A, [S.L.], v. 15, n. 1, p. 1-21. Zhejiang University Press. http://dx.doi.org/10.1631/jzus.a1300217.

Saldivar, R.E.R. (2025). Cálculo de curva de recalques superficiais longitudinais como ferramenta para acompanhamento e controle de escavação (ATO) de túneis NATM e túneis TBM-EPB em ambientes urbanos. Latin American Tunnelling Seminar - LAT 2025, São Paulo, Brazil.

Wang J., Tian N., Lin G., Feng K., Xie H.. (2024). Face failure of deep EPB shield tunnels in dry graded cobble-rich soil: A DEM study. *Tunnelling and Underground Space Technology* 147 (2024) 105622.

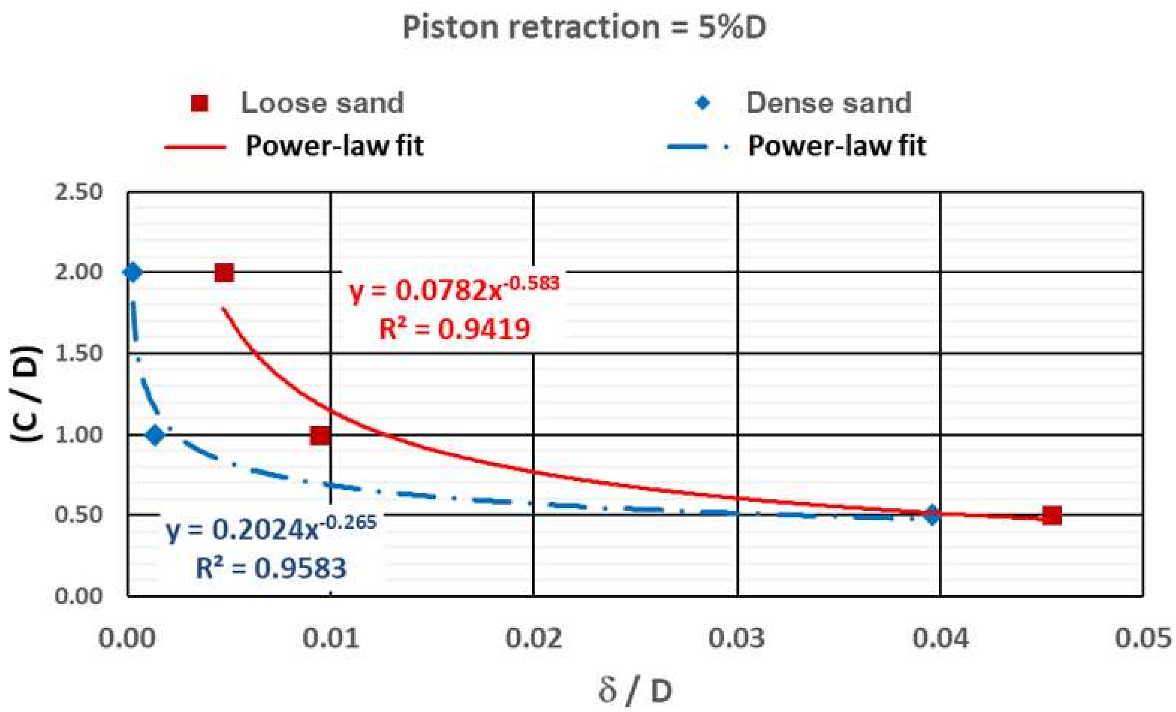

Figure 4: Relationship between surface settlement at S1 and tunnel cover depth, expressed as the cover-to-diameter ratio (C/D = 0.5,1.0, 2.0), for loose and dense sands.

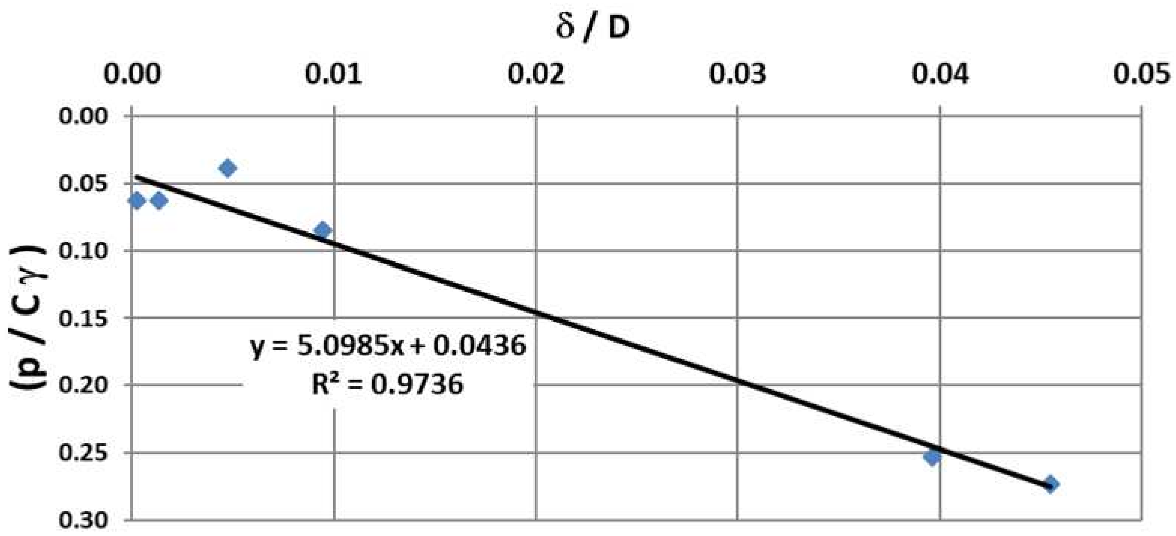

Figure 5: Relationship between surface settlement at S1 and face pressure relief at the TBM piston, accounting for tunnel geometry and soil unit weight.

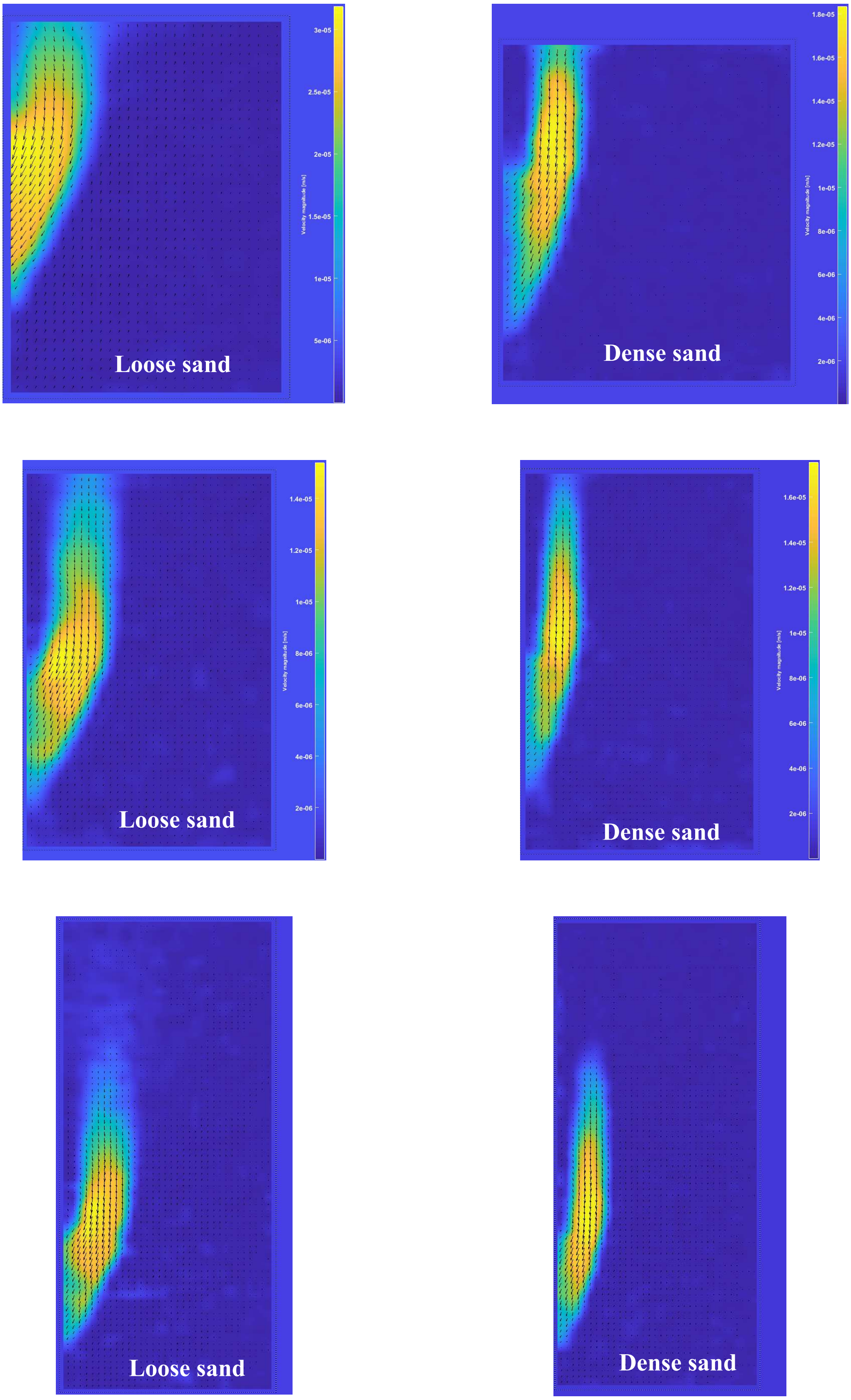

(a)

(b)

(c)

Figure 6: Displacement field mapping obtained by PIV analysis in Matlab, showing velocity vectors induced by excavation in loose and dense sands. (a) for cover-to-diameter ratio (C/D = 0.5), (b) for cover-to-diameter ratio (C/D = 1.0), (c) for cover-to-diameter ratio (C/D = 2.0)